[CANCER RESEARCH 61, 3027–3032, April 1, 2001]

Characterization of the Effect of Hyperthermia on Nanoparticle Extravasation from Tumor Vasculature[1]

Garheng Kong, Rod D. Braun, and Mark W. Dewhirst[2]

Departments of Biomedical Engineering [G. K.] and Radiation Oncology [R. D. B., M. W. D.], Duke University Medical Center, Durham, North Carolina 27710

ABSTRACT

The efficacy of novel cancer therapeutics can be hampered by inefficient delivery of agents to the tumor at effective concentrations. Liposomes have been used as a method to overcome some delivery issues and, in combination with hyperthermia, have been shown to increase drug delivery to tumors. This study investigates the effects of a range of temperatures (34–42°C) and hyperthermia treatment scheduling (time between hyperthermia and drug administration as well as between consecutive hyperthermia treatments) on the extravasation of nanoparticles (100-nm liposomes) from tumor microvasculature in a human tumor (SKOV-3 ovarian carcinoma) xenograft grown in athymic nude mouse window chambers. Under normothermic conditions (34°C) and at 39°C, nanoparticles were unable to extravasate into the tumor interstitium. From 40 to 42°C, nanoparticle extravasation increased with temperature, reaching maximal extravasation at 42°C. Temperatures higher than 42°C led to hemorrhage and stasis in tumor vessels. Enhanced nanoparticle extravasation was observed several hours after heating, decaying back to baseline at 6 h postheating. Reheating (42°C for 1 h) 8 h after an initial heating (42°C for 1 h) did not result in any increased nanoparticle extravasation, indicating development of vascular thermotolerance. The results of this study have implications for the application and scheduling of hyperthermia combined with other therapeutics (*e.g.*, liposomes, antibodies, and viral vectors) for the treatment of cancer.

INTRODUCTION

One of the dose-limiting factors in current chemotherapeutic regimens is the significant systemic toxicity associated with the treatment (1). This is largely attributable to the nonspecific nature and widespread dissemination of these compounds throughout the body. Attempts to develop targeted therapeutic agents include the utilization of antibodies, viral vectors, and drug carriers (2–4). Many of these cancer chemotherapeutic agents have been shown to be highly effective *in vitro* but not as effective *in vivo* (5). One reason for the relative lack of effectiveness of such therapeutic agents (on the order of hundreds of nanometers in size) is that they do not cross the vascular wall efficiently (6).

To overcome this delivery barrier in tumors, modification of the target environment has been attempted with various degrees of success. The use of compounds such as vascular endothelial growth factor or histamine has been shown to affect the size of particles that can be delivered to tumors (7, 8). Radiation has been shown to induce vascular endothelial growth factor expression and thus increase tumor permeability (9). HT[3] has also been used to modify the local tumor environment to increase nanoparticle delivery to tumors (10). Although classically viewed as a form of adjuvant therapy to increase the efficacy of radiation and chemotherapy, HT can be applied to augment nanoparticle delivery by increasing tumor blood flow and tumor microvascular pore size (11). At temperatures of 41–43°C, HT has been shown to increase blood flow (12) and oxygenation (13) in tumors. HT has also been shown to increase permeability of tumor vessels to antibodies (14–17), ferritin (18), Evans blue dye (19), and liposomes (20).

We now report experiments to further characterize HT's effect on nanoparticle (defined as a 100-nm liposome unless otherwise noted) extravasation from tumor vasculature. We hypothesized that (*a*) HT will enable nanoparticle extravasation from tumor vessels above a threshold temperature; (*b*) nanoparticle extravasation will be positively correlated with temperature above this threshold; (*c*) HT's effect on nanoparticle extravasation will decay over time; and (*d*) HT will lose its ability to increase nanoparticle extravasation if administered in close proximity to a previous heating.

MATERIALS AND METHODS

Nanoparticles: 100-nm Liposomes. Rho-labeled sterically stabilized long-circulating PEG liposomes were prepared by the lipid film hydration and extrusion method (21). The formulation for the liposomes was egg phosphatidylcholine:cholesterol:1,2-distearoyl-*sn*-glycero-3-phosphoethanolamine-*N*-polyethylene glycol 2000:rhodamine-labeled phosphoethanolamine in the molar ratio of 10:5:0.8:0.1 (22). The final lipid concentration after hydration was 20 mg/ml, and 100-nm liposomes were sized by multiple passes through 0.1-μm polycarbonate filters (Poretics, Livermore, CA). Liposome size was determined by dynamic light scattering using a Coulter N4 MD Submicron Particle Size Analyzer (Coulter Electronics, Hialeah, FL). All liposome preparations used in this study were 100 nm in diameter, with a narrow size distribution (95% of the liposomes were within $\pm$10 nm). One hundred-nm liposomes were chosen because they were found to be the optimal size for hyperthermia-induced extravasation in this model, based on previously published results (11).

Animal and Tumor Model. Homozygous NCr athymic nude mice (20 $\pm$ 3 g) were purchased from Taconic (Germantown, NY). Animals were housed in appropriate isolated caging with sterile rodent food, acidified water *ad libitum*, and a 12-h light/dark cycle. All protocols were approved by the Duke Institutional Animal Care and Use Committee. The athymic nude mouse dorsal skin flap window chamber model was used (23). Briefly, titanium window chambers were surgically placed on the dorsal skin flap of athymic nude mice, and a small volume ($\sim$0.1 mm^3) of tumor tissue (human ovarian carcinoma; SKOV-3) was implanted in the window chamber. After 10–14 days, the tumor was visibly well vascularized and $\sim$1–2 mm in diameter. This preparation was then used for experiments.

The permeability of tumor vasculature to nanoparticles is dependent on the tumor type (24). Some tumors have pore cutoff sizes between 400 and 600 nm (22). After initially screening several tumor types, SKOV-3, a human ovarian carcinoma was found to be highly impermeable to 100-nm liposomes under normothermic conditions. Non-tumor bearing window chamber vessels were similarly impermeable to 100-nm liposomes under normothermic conditions. Because this tumor represents a limiting case for permeability, it was chosen as the model for this study. It provides a strict model for assaying HT's ability to enable and increase permeability in tumor vessels.

Experimental Procedure. In each experiment animals were anesthetized with sodium pentobarbital (80 mg/kg; i.p.). The tail vein was cannulated for i.v. injection of liposomes during the experiment. The animal was placed on a temperature-controlled microscopic stage to maintain normal body temperature throughout the experiment. The window chamber was fixed in a specially designed HT chamber (25) that allowed for visualization of the tumor while the chamber was being heated (to 34°C, 39°C, 40°C, 41°C, or 42°C). The window

Received 8/29/00; accepted 1/29/01.

The costs of publication of this article were defrayed in part by the payment of page charges. This article must therefore be hereby marked *advertisement* in accordance with 18 U.S.C. Section 1734 solely to indicate this fact.

[1] Supported by NIH Grants CA-42745 and CA-40355 and a grant from the Celsion Corporation.

[2] To whom requests for reprints should be addressed, at Department of Radiation Oncology, Box 3455, Duke University Medical Center, Durham, NC 27719.

[3] The abbreviations used are: HT, hyperthermia; RTIA, relative tumor interstitial amount; $RTIA_{60}$, RTIA at 60 min.

chamber and tumor were allowed to reach steady state temperature (~2 min as determined by thermographic imaging) in the HT chamber before injection of liposomes. The preparation in the window chamber was observed with a 20× objective lens. A region in the preparation with steady blood flow and few obvious underlying vessels was selected as an appropriate region for analysis (26). The images of the selected region were recorded with a SIT camera (C2400-08; Hamamatsu) connected to a S-VHS video tape recorder (BV-1000; Mitsubishi). This region was first recorded under transillumination. Then, under epi-illumination with a filter set for rhodamine (H546; Zeiss), a background image of the selected region was recorded before injection of liposomes. Next, 0.2 ml of rhodamine-labeled liposomes was administered i.v. The region was recorded under epi-illumination intermittently (for 10 s every 2 min) for 60 min after the injection of liposomes.

The videotape of the experiment was analyzed with image processing software (NIH Scion Image). The fluorescent light intensities of the entire selected region and representative vascular regions were measured at serial time points. The relative fluorescent light intensities of the vascular and interstitial components were determined as described by Wu *et al.* (26). All light intensities were normalized to the initial vascular light intensity in the region after injection of liposomes. Vascular volumes for all of the experimental groups were not statistically different (data not shown). Because the light intensity is proportional to the number of particles present, the data are presented as RTIA in this paper as previously described (11). RTIA values taken at 60 min are defined as $RTIA_{60}$.

Experimental Groups. Each experimental group had six mice, and all of them used 100-nm nanoparticles (rhodamine-labeled liposomes). Because HT at 42°C has previously been shown to have some effect on nanoparticle delivery (11), the temperature dependence of nanoparticle extravasation was determined by performing the experimental procedure described above at 34°C (normal s.c. skin temperature of mice; Ref. 20), 39°C, 40°C, 41°C, and 42°C (this was the highest temperature group because of significant tumor hemorrhage seen at 43°C). To evaluate the time frame over which HT affects nanoparticle extravasation, tumors were heated at 42°C for 1 h. Then nanoparticles were administered either 2, 4, or 6 h after HT under normothermic conditions (34°C), and intravital microscopy was performed. To evaluate whether there is evidence for thermotolerance to HT-induced nanoparticle extravasation, tumors were heated to 42°C for 1 h. Eight h later, animals were reanesthetized, and nanoparticles were administered while the tumor was again heated to 42°C for 1 h.

Statistics. Changes in RTIA were summarized by averaging data from individual animals in each group. Statistical significance between experimental groups was determined using the Mann-Whitney *U* test. Two quantities were regarded as statistically significantly different if $P < 0.05$.

RESULTS

General Description. After identifying an appropriate region within the tumor by transillumination, epi-illumination was used to measure the extravasation of liposomes under normothermic and hyperthermic conditions. The typical preparation, seen with epi-illumination, is shown in Fig. 1 using a filter set for the rhodamine label. In general, the fluorescent signal indicating labeled particles appeared in preparations ~10 s after injection and became stable within ~30 s. Throughout the 60-min observation, the tumor blood vessels retained fluorescent signal (Fig. 1), consistent with previous sterically stabilized liposome pharmacokinetic data (27, 28). Perivascular fluorescent spots usually indicated initial liposome extravasation that later became more diffuse and spread throughout the tumor interstitium (Fig. 1*E*). These initial fluorescent spots were heterogeneously distributed along the vessel. This suggests that the leakage pattern of liposomes from the tumor vessels is dependent on heterogeneously spaced and/or sized pores along the tumor vessel wall (29).

Temperature Dependence of HT-induced Nanoparticle Extravasation. The temperature range tested was 34–42°C because this represented the important physiological and therapeutic temperature range. Under normothermic conditions, the tumor temperature is 34°C, and above 42°C the tumor vessels hemorrhaged and collapsed. At 34°C and 39°C (Fig. 1, *A* and *B*, respectively), nanoparticles did not extravasate into the tumor interstitium, with $RTIA_{60}$s ~ 0 (Fig. 2). From 40 to 42°C, nanoparticle extravasation (Fig. 1, *C–E*) increased with temperature with $RTIA_{60}$s of 0.46, 0.94, and 1.53, respectively (Fig. 2). The $RTIA_{60}$s at 41°C and 42°C were not statistically different from each other ($P \approx 0.1$), but were both significantly higher than the $RTIA_{60}$s at 34°C, 39°C, or 40°C ($P < 0.03$).

Decay of HT-induced Nanoparticle Extravasation. Because little work has been focused on the time frame over which HT affects nanoparticle extravasation, we examined nanoparticle extravasation (under normothermic conditions) at different time points after HT at 42°C for 1 h (Fig. 3). Two h after the end of HT, the $RTIA_{60}$ was 0.70 (Fig. 4), still significantly above baseline ($P < 0.01$), though lower than the $RTIA_{60}$ of 1.53 seen with HT (42°C for 1 h) given simultaneously. Four h after the end of HT (42°C for 1 h; Fig. 3*B*), the $RTIA_{60}$ was reduced to 0.32, but this was still above baseline ($P < 0.01$). By 6 h after the end of HT (42°C for 1 h; Fig. 3*C*), no nanoparticle extravasation was evident, $RTIA_{60}$ was ~0 (Fig. 4), and

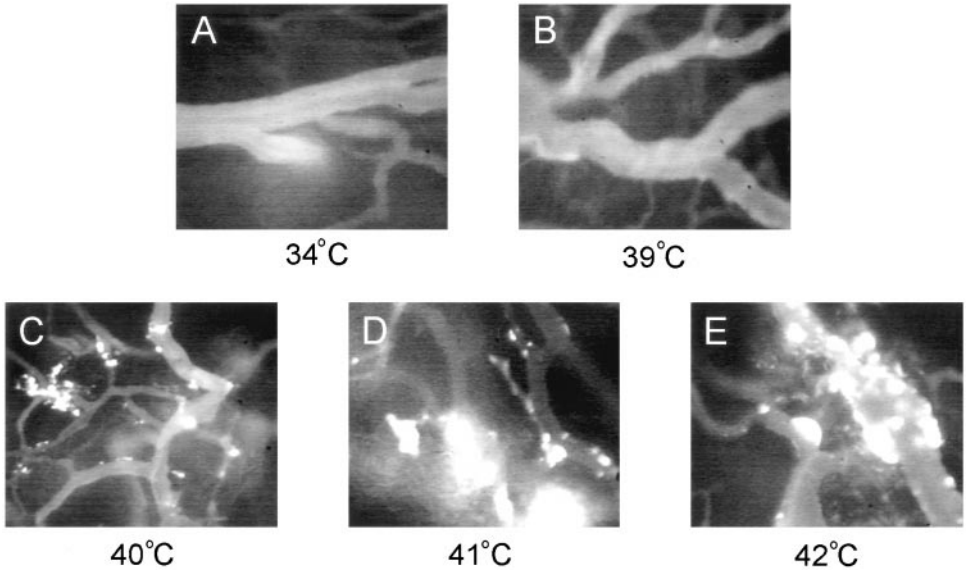

Fig. 1. Extravasation of nanoparticles from tumor vessels at 60 min after injection at different temperatures. *A*, 34°C; *B*, 39°C; *C*, 40°C; *D*, 41°C; *E*, 42°C. Minimal extravasation of nanoparticles was seen at 34°C throughout the 60-min experiment. At 42°C, focal perivascular fluorescent spots developed that increased in size and became more diffuse.

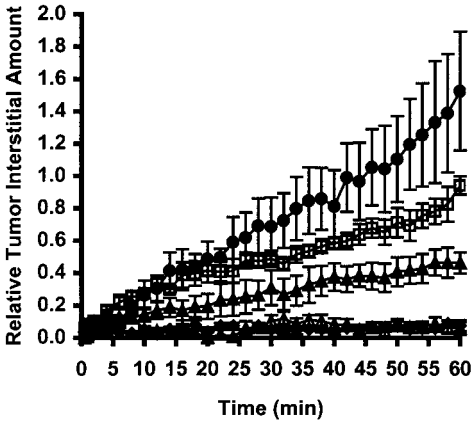

Fig. 2. HT-induced extravasation of nanoparticles after 60 min at different temperatures. The RTIA at 34°C (△), 39°C (♦), 40°C (▲), 41°C (□), and 42°C (●). The largest HT enhancement of extravasation was seen at 42°C. Values are mean and SE ($n = 6$ for each temperature).

it appeared that the tumor vasculature had returned to baseline impermeability—similar to no HT at all.

Effect of Previous HT on HT-induced Nanoparticle Extravasation. In this model, HT's effect on liposome extravasation decayed after 6 h. To determine whether the enhanced extravasation could be repeated, a second set of tumors was heated twice: 42°C for 1 h and 8 h after being heated at 42°C for 1 h. For tumors that had received HT 8 h prior, HT did not increase liposome extravasation into the tumor interstitium (Figs. 5 and 6). The overall effect was similar to that seen for liposome extravasation at 34°C (Figs. 1*A* and 2).

DISCUSSION

Mechanism of HT-induced Nanoparticle Extravasation. HT has been previously shown to increase the permeability of already hyperpermeable tumor vessels (14–19). The precise mechanism behind HT-induced nanoparticle extravasation has not been clearly elucidated, but there are several reasonable explanations that have been proposed. The leading hypothesis involves the concept of a "pore cutoff size." Functional and structural studies have shown that large pores exist in tumor vessels that would facilitate nanoparticle extravasation (6). Additionally, the degree of nanoparticle extravasation from tumor vessels is based on size, and above a certain threshold of nanoparticle size, no extravasation is seen (22). It has been proposed that HT-induced nanoparticle extravasation may occur because of pore cutoff size augmentation (11). This may result from HT's ability to disaggregate the endothelial cell cytoskeleton and cause morphological changes that appear to "shrink" the cell (30–32). These morphological changes would allow larger pores to be formed between endothelial cells and translate into enhanced nanoparticle extravasation (19, 20). This phenomenon has been supported by electron microscopic studies, which showed large breaches in the vascular wall after HT (33). Other explanations for HT-induced nanoparticle extravasation include modification of tumor blood flow (12, 34), increased intravascular pressure (35–37), and decreased tumor interstitial fluid pressure (38). Previous studies in this tumor model have shown that nanoparticles below the pore cutoff size, which extravasate to a large degree under normothermic conditions, did not show increased extravasation with HT (11). If blood flow, interstitial fluid pressure, or intravascular pressure were significant factors in increasing nanoparticle extravasation, an increased extravasation should have been seen for these smaller nanoparticles. Although these factors are less likely to account for the significant differences in extravasation achieved (*e.g.,* no extravasation *versus* significant extravasation) with and without HT, they may play roles in modifying the degree of extravasation. As will be discussed below, the data for this study appear to be the most consistent with the model that HT affects the endothelial cytoskeletal structure, leading to changes in pore cutoff size.

Temperature Dependence of HT-induced Nanoparticle Extravasation. Under normothermic conditions (34°C), no nanoparticle extravasation was seen (Figs. 1*A* and 2). This result was expected because the SKOV-3 tumor line was chosen for its impermeability to nanoparticles (on the order of 100 nm) without HT. With mild HT, 39°C, no extravasation was achieved (Figs. 1*B* and 2). We chose 39°C as the initial temperature to test for extravasation because increases in tumor oxygenation (13) and blood flow (39) have been demonstrated at this temperature. At 40°C, nanoparticle extravasation was first achieved ($RTIA_{60} = 0.46$), and it continued to increase with temperature up to 42°C ($RTIA_{60} = 1.53$). Thus, the threshold temperature for increased extravasation in this model was between 39°C and 40°C. Beyond 42°C the tumor vessels hemorrhaged and collapsed after several minutes of exposure to HT (this occurred in all four tumors that were tested at 43°C). There was a tight linear relationship between $RTIA_{60}$ and temperature in the range of 39–42°C (Fig. 7), with a correlation coefficient of 0.99. These results can be explained by the mechanism of endothelial cell shrinking and subsequent increased tumor vessel permeability. As temperature increases, tumor endothelial cytoskeletal proteins may disaggregate affording pore sizes between endothelial cells to increase. Tumor vasculature may be more susceptible to HT because of a different endothelial architecture (40). Additionally, increased intravascular pressure or tumor blood flow attributable to HT could add to the effect of larger tumor vessel pores. However, to significantly augment nanoparticle extravasation in this situation, it is necessary to increase pore cutoff size.

Although no studies have examined the incremental temperature dependence of nanoparticle extravasation, the effect of different temperatures on extravasation of various nanoparticles has been studied and yielded similar results. In a hepatic tumor model, Gnant *et al.* (41) have shown no increased albumin permeability in tumor vessels at 39°C but increased permeability at 41°C. Lefor *et al.* (19) in a different tumor model saw no increased albumin permeability at 40°C but found a significant increase in permeability at 43°C . In the mild hyperthermic range of 38.5–41.5°C, tumor oxygenation and perfusion have been shown to increase as temperature increases, but the oppo-

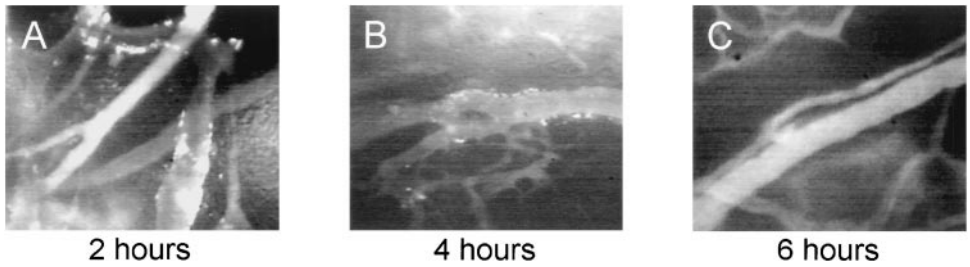

Fig. 3. Extravasation of nanoparticles under normothermic conditions at different time points after HT (42°C for 1 h). Images depict 60 min after nanoparticle administration. Nanoparticles administered at (*A*) 2 h after the end of HT, (*B*) 4 h after the end of HT, and (*C*) 6 h after the end of HT. Six h after the end of HT, no extravasation was seen.

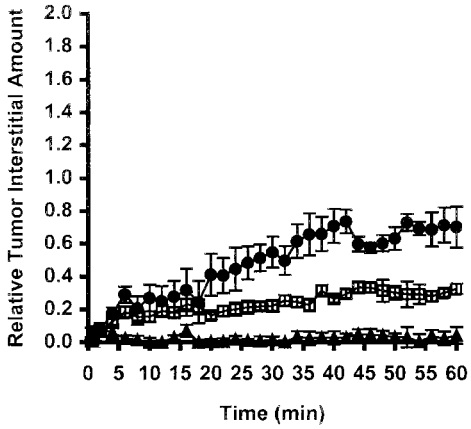

Fig. 4. HT-induced extravasation of nanoparticles under normothermic conditions after heating at 42°C for 1 h. The RTIA 2 h after the end of HT(●), 4 h after the end of HT (□), and 6 h after the end of HT (▲). Values are mean and SE (n = 6 for each temperature).The mean and SE are shown (n = 6 for each group).

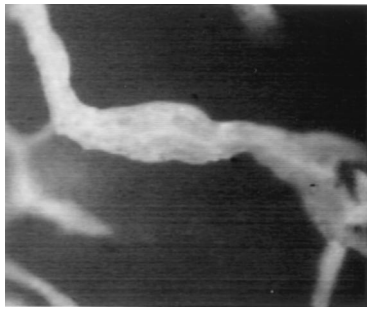

Fig. 5. Lack of nanoparticle extravasation at 42°C in a tumor that was heated 8 h prior at 42°C for 1 h. This image is after 60 min of the second HT treatment.

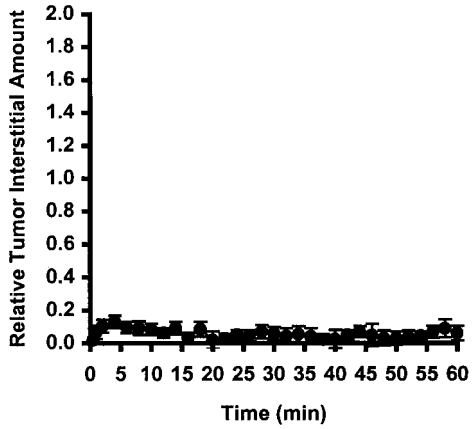

Fig. 6. The RTIA achieved at 42°C after being heated 8 h prior at 42°C for 1 h. The RTIA profile is similar to that of no HT at all. Values are mean and SE (n = 6 for each temperature).

site happens at higher temperatures (13, 42). We chose to study the range of 39–42°C because of the relevance to current clinical HT treatments. In many models, similar to the results in this study, an upper threshold limit (43–45°C) was seen above which HT caused significant vascular damage, stasis, and decreased extravasation (43–46). For clinically relevant temperatures (39–42°C), HT does increase extravasation in the tumor.

Decay of HT-induced Nanoparticle Extravasation. The ability of HT to enable nanoparticle extravasation decayed over 6 h in this model (Figs. 3 and 4). The extravasation seen 2 h after HT was still significant ($RTIA_{60}$ = 0.70) but much less than the extravasation achieved during 1 h of HT ($RTIA_{60}$ = 1.53). Six h after HT, nanoparticle extravasation had returned to baseline, *i.e.*, almost no extravasation was seen. The decay of extravasation post-HT was also highly linear (Fig. 8). The transient nature of HT-induced nanoparticle extravasation suggests a reversible mechanism that occurs with HT and reverts once the heat is removed. This would argue against permanent vascular damage as the mechanism in this temperature range. Although transient, the effects of HT on extravasation extend to several hours after administration, which make changes in physiological parameters such as blood flow or intravascular pressure less likely an explanation. The time frame and nature of the results presented here are consistent with protein disaggregation and reassembly. Microtubules of the cytoskeleton have been shown to disaggregate during HT and reaggregate during subsequent incubation at 37°C (30). More specifically, HT (43°C for 1 h) treatment of human umbilical vein endothelial cells has been shown to cause reversible loss of actin filaments that may contribute to increased "leakage" of tumor microvasculature (47). Cytoskeletal recovery after HT occurs over a similar time frame (~hours) as the decay of HT-induced extravasation (48, 49). This is also coincident with the expression and activity of heat shock proteins (~hours) that facilitate protein recovery and reassembly (50). Thus, the decay of extravasation may be linked to cytoskeletal recovery post-HT and increased heat shock protein activity.

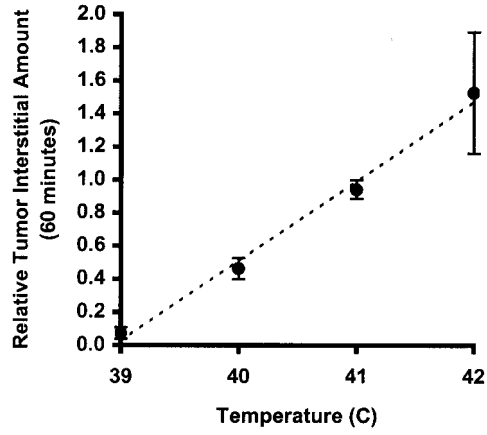

Fig. 7. Correlation of $RTIA_{60}$ as a function of temperature. The correlation coefficient was 0.99 ($y = 0.48x + 18.82$). Values are mean and SE (n = 6 for each temperature).

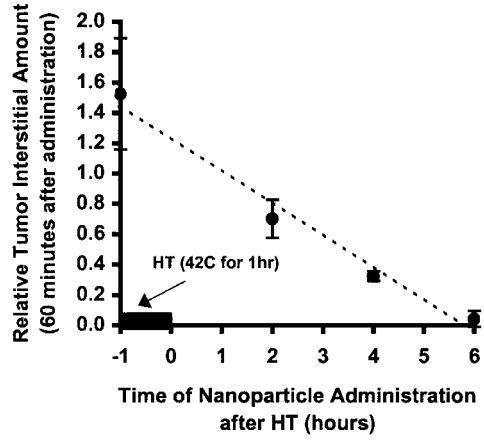

Fig. 8. Correlation of $RTIA_{60}$ as a function of time of nanoparticle administration after HT (42°C for 1 h). The correlation coefficient was 0.99 ($y = -0.21x + 1.23$). Values are mean and SE (n = 6 for each temperature).

Effect of Previous HT on HT-induced Nanoparticle Extravasation. We chose to reheat tumors after an 8-h interval for two main reasons: (*a*) the extravasation of nanoparticles returned to baseline 6 h after HT; thus, no residual extravasation would be present; and (*b*) thermotolerance (51) has been shown to occur rather soon (~hours; Refs. 52 and 53) after administration of HT, so any possible effects from thermotolerance might be active at that time. Thermotolerance can be generally defined as increased resistance to HT, usually developed after an initial exposure of HT (54).

Tumors that were given HT 8 h prior did not respond to HT again. No HT-induced nanoparticle extravasation was seen (Figs. 5 and 6). The most likely explanation for this is the development of thermotolerance, in the case of nanoparticle extravasation, vascular thermotolerance (55). Thermotolerance has been shown to develop in multiple tumor models at similar thermal doses as described here (42°C for 1 h; Refs. 56–59). More specifically, vascular thermotolerance has been shown to develop within 5 h of HT (42.5°C for 1 h), peak at 18 h, and decay over several days (53). In this situation, thermotolerance was determined based on vascular damage and decreased blood flow as opposed to extravasation. Besides this group of studies, there has been little work examining vascular thermotolerance. As the endothelial cells of the tumor vessels develop thermotolerance, subsequent HT may become less effective at disaggregating the cytoskeletal structures that result in enhanced extravasation. Although the development and decay of thermotolerance varies with the tissue or tumor type, most *in vivo* models have shown that thermotolerance has largely disappeared after 7 days (57). Development of thermotolerance has been correlated with heat shock protein activity (60, 61), and heat shock protein activity develops over a similar time frame (62) as the vascular thermotolerance seen in this model. Thus, HT may initiate heat shock protein activity in tumor endothelial cells that makes the cytoskeletal proteins more resistant to subsequent heating, which ultimately results in retained vascular integrity and reduced nanoparticle extravasation.

Implications for Therapy. HT has been shown to increase the delivery of therapeutic nanoparticles such as liposomes and antibodies (10, 17). This ability has not been well characterized with regard to optimal temperature and scheduling of HT and drug administration. Although many have believed that therapeutic HT required temperatures greater than 43°C, the results of this study indicate that temperatures several degrees lower can lead to increased drug delivery. Thus mild heating of a tumor (*e.g.*, goal of 40–42°C) conveys the greatest benefit with regard to drug delivery with nanoparticles. Given the nonuniform nature of most HT treatments, it appears that combination HT and nanoparticle drug delivery would result in various degrees of tumor drug concentration dependent on the temperature at the local region in the tumor.

Mild HT's ability to enhance extravasation opens the possibility of a twofold mechanism for combination HT and liposome therapy. Thermosensitive liposomes, which release drug in the mild HT range of 39–41°C (63), could be given in combination with local HT at 41°C. These liposomes would preferentially extravasate into the tumor at 41°C and also release their contents, leading to increased liposomal delivery and drug release in the tumor.

The results of this study also highlight the importance of administering HT and therapeutic nanoparticles together or temporally as closely as logistically possible. With an effective time frame of <6 h in this model, HT given too far ahead of the drug results in reduced efficacy of the intervention. Because long-circulating liposomes have half-lives that are much longer than the HT-induced extravasation (27), it may be logistically more reasonable in a hospital to administer liposomes first and then HT. Additionally, combination treatments with HT aimed to exploit HT-induced nanoparticle extravasation need to be adequately spaced to allow for any thermotolerance that has been developed to decay before the subsequent treatment. Thermotolerance has been thought to be the reason that some clinical trials have shown that six heat treatments were no more effective than two heat treatments (64), although other clinical data do not support that hypothesis (65).

The tumor model used in this study was chosen because it was impermeable to the 100-nm nanoparticle extravasation at normothermia and represented a limiting case. This represents an important clinical situation where therapeutic agents of this size are normally unable to cross the tumor vascular wall. Of course there are other tumor types that are more permeable to nanoparticles. In such tumors, as permeability increases, the role of convective forces might become more important, and factors such as intravascular pressure and blood flow would impact overall nanoparticle extravasation. Additionally, HT's ability to augment pore cutoff size may have a smaller relative effect than in the situation of the SKOV-3 model. The exact effect of HT on nanoparticle extravasation in a highly permeable tumor model is difficult to predict because it would be a function of many different factors.

Overall, the efficacy of combination HT and therapeutic nanoparticle therapy is highly dependent on the thermal dose, scheduling, and previous HT. Examining other tumor models and different thermal doses could expand the results of this study. Determining when HT-induced extravasation returns and how to accelerate the process after a previous heating may be important in the design of an optimal treatment regimen.

ACKNOWLEDGMENTS

We thank Ken Schopfer for experimental help, Dr. David Needham for use of facilities, and Mike Grenn for help with hyperthermia chamber calibration.

REFERENCES

1. Lowenthal, R. M., and Eaton, K. Toxicity of chemotherapy. Hematol Oncol Clin North Am., *10:* 967–990, 1996.
2. Allen, T. M. Liposomes: opportunities in drug delivery. Drugs, *54:* 8–14, 1997.
3. Weiner, L. M. Monoclonal antibody therapy of cancer. Semin. Oncol., *26:* 43–51, 1999.
4. Vile, R. G., Russell, S. J., and Lemoine, N. R. Cancer gene therapy: hard lessons and new courses. Gene Ther., *7:* 2–8, 2000.
5. Jain, R. K. Barriers to drug delivery in solid tumors. Sci. Am., *271:* 58–65, 1994.
6. Yuan, F. Transvascular drug delivery in solid tumors. Semin. Radiation Oncol., *8:* 164–175, 1998.
7. Yuan, F., Leunig, M., Huang, S. K., Berk, D. A., Papahadjopoulos, D., and Jain, R. K. Microvascular permeability and interstitial penetration of sterically stabilized (stealth) liposomes in a human tumor xenograft. Cancer Res., *54:* 3352–3356, 1994.
8. Monsky, W. L., Fukumura, D., Gohongi, T., Ancukiewcz, M., Weich, H. A., Torchilin, V. P., Yuan, F., and Jain, R. K. Augmentation of transvascular transport of macromolecules and nanoparticles in tumors using vascular endothelial growth factor. Cancer Res., *16:* 4129–4135, 1999.
9. Gorski, D. H., Beckett, M. A., Jaskowiak, N. T., Calvin, D. P., Mauceri, H. J., Salloum, R. M., Seetharam, S., Koons, A., Hari, D. M., Kufe, D. W., and Weichselbaum, R. R. Blockage of the vascular endothelial growth factor stress response increases the antitumor effects of ionizing radiation. Cancer Res., *59:* 3374–3378, 1999.
10. Kong, G., and Dewhirst, M. W. Hyperthermia and liposomes. Int. J. Hyperth., *15:* 345–370, 1999.
11. Kong, G., Braun, R. D., and Dewhirst, M. W. Hyperthermia enables tumor-specific nanoparticle delivery: effect of particle size. Cancer Res., *60:* 4440–4445, 2001.
12. Karino, T., Koga, S., and Maeta, M. Experimental studies of the effects of local hyperthermia on blood flow, oxygen pressure and pH in tumors. Jpn. J. Surg., *18:* 276–283, 1988.
13. Horsman, M. R., and Overgaard, J. Can mild hyperthermia improve tumour oxygenation? Int. J. Hyperth., *13:* 141–147, 1997.
14. Cope, D., Dewhirst, M., Friedman, H., Bigner, D., and Zalutsky, M. Enhanced delivery of a monoclonal antibody $F(ab')^2$ fragment to subcutaneous human glioma xenografts using local hyperthermia. Cancer Res., *50:* 1803–1809, 1990.
15. Hosono, M. N., Hosono, M., Endo, K., Ueda, R., and Onoyama, Y. Effect of hyperthermia on tumor uptake of radiolabeled anti-neural cell adhesion molecule antibody in small-cell lung cancer xenografts. J. Nucl. Med., *35:* 504–509, 1994.
16. Schuster, J., Zalutsky, M., Noska, M., Dodge, R., Friedman, H., Bigner, D., and Dewhirst, M. Hyperthermic modulation of radiolabelled antibody uptake in a human glioma xenograft and normal tissues. Int. J. Hyperth., *11:* 59–72, 1995.

17. Hauck, M., Coffin, D., Dodge, R., Dewhirst, M., Mitchell, J., and Zalutsky, M. A local hyperthermia treatment which enhances antibody uptake in a glioma xenograft model does not affect tumour interstitial fluid pressure. Int. J. Hyperth., *13:* 307–316, 1997.
18. Fujiwara, K., and Watanabe, T. Effects of hyperthermia, radiotherapy and thermoradiotherapy on tumor microvascular permeability. Acta Pathol. Jpn., *40:* 79–84, 1990.
19. Lefor, A., Makohon, S., and Ackerman, N. The effects of hyperthermia on vascular permeability in experimental liver metastasis. J Surg Oncol., *28:* 297–300, 1985.
20. Gaber, M. H., Wu, N. Z., Hong, K., Huang, S. K., Dewhirst, M. W., and Papahadjopoulos, D. Thermosensitive liposomes: extravasation and release of contents in tumor microvascular networks. Int. J. Radiat. Oncol. Biol. Phys., *36:* 1177–1187, 1996.
21. Hope, M. J., Bally, M. B., Webb, G., and Cullis, P. R. Production of large unilamellar vesicles by a rapid extrusion procedure. Characterization of size distribution, trapped volume and ability to maintain a membrane potential. Biochim. Biophys. Acta, *812:* 55–65, 1985.
22. Yuan, F., Dellian, M., Fukumura, D., Leunig, M., Berk, D. A., Torchilin, V., and Jain, R. K. Vascular permeability in a human tumor xenograft: molecular size dependence and cutoff size. Cancer Res., *55:* 3752–3756, 1995.
23. Huang, Q., Shan, S., Braun, R. D., Lanzen, J., Anyarambhatla, G., Kong, G., Borelli, M., Corry, P., Dewhirst, M. W., and Li, C. Y. Noninvasive visualization of tumors in rodent dorsal skin window chambers. Nat. Biotechnol., *17:* 1033–1035, 1999.
24. Yuan, F., Salehi, H. A., Boucher, Y., Vasthare, U. S., Tuma, R. F., and Jain, R. K. Vascular permeability and microcirculation of gliomas and mammary carcinomas transplanted in rat and mouse cranial windows. Cancer Res., *54:* 4564–4568, 1994.
25. Gross, J. F., Roemer, R., Dewhirst, M. W., and Meyer, M. A uniform thermal field in a hyperthermia chamber for microvascular studies. Int. J. Heat Mass Transf., *25:* 1313–1320, 1982.
26. Wu, N. Z., Klitzman, B., Rosner, G., Needham, D., and Dewhirst, M. Measurement of material extravasation in microvascular networks using fluorescence videomicroscopy. Microvasc. Res., *46:* 231–253, 1993.
27. Allen, T. M., Hanser, C., Redemann, C., and Yau-Young, A. Liposomes containing synthetic derivatives of poly (ethylene glycol) show prolonged circulation half-lives *in vivo*. Biochim. Biophys. Acta., *1066:* 29–36, 1991.
28. Lasic, D. D., and Martin, F. J. Stealth Liposomes. Boca Raton, FL: CRC, 1995.
29. Wu, N. Z., Da, D., Rudoll, T. L., Needham, D., Whorton, A. R., and Dewhirst, M. W. Increased microvascular permeability contributes to preferential accumulation of Stealth liposomes in tumor tissue. Cancer Res., *53:* 3765–3770, 1993.
30. Lin, P. S., Turi, A., Kwock, L., and Lu, R. C. Hyperthermia effect on microtubule organization. NCI Monogr., *61:* 57–60, 1982.
31. Glass, J., DeWitt, R., and Cress, A. Rapid loss of stress fibers in Chinese hamster ovary cells after hyperthermia. Cancer Res., *45:* 258–262, 1985.
32. Dermietzel, R., and Streffer, C. The cytoskeleton and proliferation of melanoma cells under hyperthermal conditions. A correlative double immuno-labeling study. Strahlenther. Onkol., *168:* 593–602, 1992.
33. Clark, A., Robins, H., Vorpahl, J., and Yatvin, M. Structural changes in murine cancer associated with hyperthermia and lidocaine. Cancer Res., *43:* 1716–1723, 1983.
34. Song, C., Lokshina, A., Rhee, J., Patten, M., and Levitt, S. Implication of blood flow in hyperthermic treatment of tumors. IEEE Trans. Biomed. Eng., *31:* 9–16, 1984.
35. Page, R. L., Meyer, R. E., Thrall, D. E., and Dewhirst, M. W. Cardiovascular and metabolic response of tumour-bearing dogs to whole body hyperthermia. Int. J. Hyperth., *3:* 513–525, 1987.
36. Kruger, W., Mayer, W. K., Schaefer, C., Stohrer, M., and Vaupel, P. Acute changes of systemic parameters in tumour-bearing rats, and of tumour glucose, lactate, and ATP levels upon local hyperthermia and/or hyperglycaemia. J. Cancer Res. Clin. Oncol., *117:* 409–415, 1991.
37. Matsuoka, H., Furusawa, M., Tomoda, H., Seo, Y., and Sugimachi, K. Efficacy of indomethacin pretreatment with regional hyperthermia for treating upper abdominal malignancies. Int. J. Hyperth., *11:* 169–171, 1995.
38. Leunig, M., Goetz, A. E., Dellian, M., Zetterer, G., Gamarra, F., Jain, R. K., and Messmer, K. Interstitial fluid pressure in solid tumors following hyperthermia: possible correlation with therapeutic response. Cancer Res., *52:* 487–490, 1992.
39. Vaupel, P., Ostheimer, K., and Muller-Klieser, W. Circulatory and metabolic responses of malignant tumors during localized hyperthermia. J. Cancer Res. Clin. Oncol., *98:* 15–29, 1980.
40. Fajardo, L. F., Schreiber, A. B., Kelly, N. I., and Hahn, G. M. Thermal sensitivity of endothelial cells. Radiat. Res., *103:* 276–285, 1985.
41. Gnant, M. F., Noll, L. A., Terrill, R. E., Wu, P. C., Berger, A. C., Nguyen, H. Q., Lans, T. E., Flynn, B. M., Libutti, S. K., Bartlett, D. L., and Alexander, H. R., Jr. Isolated hepatic perfusion for lapine liver metastases: impact of hyperthermia on permeability of tumor neovasculature. Surgery, *126:* 890–899, 1999.
42. Vujaskovic, Z., Poulson, J. M., Gaskin, A. A., Thrall, D. E., Page, R. L., Charles, H. C., MacFall, J. R., Brizel, D. M., Meyer, R. E., Prescott, D. M., Samulski, T. V., and Dewhirst, M. W. Temperature-dependent changes in physiologic parameters of spontaneous canine soft tissue sarcomas after combined radiotherapy and hyperthermia treatment. Int. J. Radiat. Oncol. Biol. Phys., *46:* 179–185, 2000.
43. Eddy, H. A. Alterations in tumor microvasculature during hyperthermia. Radiology, *137:* 515–521, 1980.
44. Dudar, T., and Jain, R. Differential response of normal and tumor microcirculation to hyperthermia. Cancer Res., *44:* 605–612, 1984.
45. Nishimura, Y., Hiraoka, M., Jo, S., Akuta, K., Yukawa, Y., Shibamoto, Y., Takahashi, M., and Abe, M. Microangiographic and histologic analysis of the effects of hyperthermia on murine tumor microvasculature. Int. J. Radiat. Oncol. Biol. Phys., *15:* 411–420, 1988.
46. Moriyama, E. Cerebral blood flow changes during localized hyperthermia. Neurol. Med-Chirur., *30:* 923–929, 1990.
47. Lin, P. S., Ho, K. C., Sung, S. J., and Gladding, J. Effect of tumour necrosis factor, heat, and radiation on the viability and microfilament organization in cultured endothelial cells. Int. J. Hyperth., *8:* 667–677, 1992.
48. Knox, J. D., Mitchel, R. E., and Brown, D. L. Effects of hyperthermia on microtubule organization and cytolytic activity of murine cytotoxic T lymphocytes. Exp. Cell Res., *194:* 275–283, 1991.
49. Yang, H., Lauzon, W., and Lemaire, I. Effects of hyperthermia on natural killer cells: inhibition of lytic function and microtubule organization. Int. J. Hyperth., *8:* 87–97, 1992.
50. Gill, R. R., Gbur, C. J., Jr., Fisher, B. J., Hess, M. L., Fowler, A. A., 3rd, Kukreja, R. C., and Sholley, M. M. Heat shock provides delayed protection against oxidative injury in cultured human umbilical vein endothelial cells. J. Mol. Cell. Cardiol. *30:* 2739–2749, 1998.
51. Henle, K. J., Karamuz, J. E., and Leeper, D. B. Induction of thermotolerance in Chinese hamster ovary cells by high (45 degrees) or low (40 degrees) hyperthermia. Cancer Res., *38:* 570–574, 1978.
52. Urano, M. Kinetics of thermotolerance in normal and tumor tissues: a review. Cancer Res., *46:* 474–482, 1986.
53. Song, C. W., Lin, J. C., Chelstrom, L. M., and Levitt, S. H. The kinetics of vascular thermotolerance in SCK tumors of A/J mice. Int. J. Radiat. Oncol. Biol. Phys., *17:* 799–802, 1989.
54. Jozwiak, Z. Involvement of heat shock proteins and cellular membranes in the development of thermotolerance. Arch. Immunol. Ther. Exp., *42:* 247–252, 1994.
55. Song, C. W., Patten, M. S., Chelstrom, L. M., Rhee, J. G., and Levitt, S. H. Effect of multiple heatings on the blood flow in RIF-1 tumours, skin and muscle of C3H mice. Int. J. Hyperth., *3:* 5355–5345, 1987.
56. Kamura, T., Nielsen, O. S., Overgaard, J., and Andersen, A. H. Development of thermotolerance during fractionated hyperthermia in a solid tumor in vivo. Cancer Res., *42:* 1744–1748, 1982.
57. Rofstad, E. K., and Brustad, T. Development of thermotolerance in a human melanoma xenograft. Cancer Res., *44:* 525–530, 1984.
58. Meyer, J. L., Van Kersen, I., Becker, B., and Hahn, G. M. The significance of thermotolerance after 41 degrees C hyperthermia: *in vivo* and *in vitro* tumor and normal tissue investigations. Int. J. Radiat. Oncol. Biol. Phys., *11:* 973–981, 1985.
59. Asaumi, J., Kawasaki, S., Kuroda, M., Takeda, Y., and Hiraki, Y. Thermosensitivity and thermotolerance in the Adriamycin-resistant strain of Ehrlich ascites tumor cells. Anticancer Res., *16:* 2569–2573, 1996.
60. Li, G. C., and Mak, J. Y. Induction of heat shock protein synthesis in murine tumors during the development of thermotolerance. Cancer Res., *45:* 3816–3824, 1985.
61. Li, G. C., and Mak, J. Y. Re-induction of hsp70 synthesis: an assay for thermotolerance. Int. J. Hyperth., *5:* 389–403, 1989.
62. Ikeda, T., Ikenoue, T., Xia, X. Y., and Xia, Y. X. Important role of 72-kd heat shock protein expression in the endothelial cell in acquisition of hypoxic-ischemic tolerance in the immature rat. Am. J. Obstet. Gynecol., *182:* 380–386, 2000.
63. Anyarambhatla, G. R., and Needham, D. Enhancement of the phase transition permeability of DPPC liposomes by incorporation of MPPC: a new temperature-sensitive liposome for use with mild hyperthermia. J. Liposome Res., *9:* 499–514, 1999.
64. Kapp, D. S., Petersen, I. A., Cox, R. S., Hahn, G. M., Fessenden, P., Prionas, S. D., Lee, E. R., Meyer, J. L., Samulski, T. V., and Bagshaw, M. A. Two or six hyperthermia treatments as an adjunct to radiation therapy yield similar tumor responses: results of a randomized trial. Int. J. Radiat. Oncol. Biol. Phys., *19:* 1481–1495, 1990.
65. Leopold, K. A., Harrelson, J., Prosnitz, L., Samulski, T. V., Dewhirst, M. W., and Oleson, J. R. Preoperative hyperthermia and radiation for soft tissue sarcomas: advantage of two *vs* one hyperthermia treatments per week. Int. J. Radiat. Oncol. Biol. Phys., *16:* 107–115, 1989.